UNIVERSITY OF CALIFORNIA SAN DIEGO

Modeling Neurodevelopmental Ethanol Exposure

A thesis submitted in partial satisfaction of the requirements
for the degree Master of Science

in

Biology

by

Justin Alan Truong

Committee in charge:

Professor Alysson Muotri Chair
Professor Brenda Bloodgood Co-chair
Professor Stacey Glasgow

2021

The thesis of Justin Alan Truong is approved, and it is acceptable in quality and form for publication on microfilm and electronically:

University of California San Diego

2021

DEDICATION

In recognition of extensive mentorship, guidance, and collaboration, this master's thesis is dedicated to Cleber Trujillo, Timothy Tran, Ryan Szeto, Jason Adams, and Alysson Muotri. In recognition of the utmost fostering of one's academic and professional scientific growth and of indispensable assistance, advice, and altruism, this master's thesis is dedicated to the Muotri Lab members.

TABLE OF CONTENTS

LIST OF FIGURES

LIST OF TABLES

ACKNOWLEDGEMENTS

The Introduction, Material and Methods, and Results section with corresponding figures, in part, contain or are inspired by manuscript components submitted for publication; the material may appear in Life Science Alliance, 2022, Jason W. Adams, Priscilla D. Negraes, Justin Truong, Timothy Tran, Ryan Szeto, Carmen Teodorof, Stephen A. Spector, Miguel Del Campo, Kenneth L. Jones, Alysson R. Muotri and Cleber A. Trujillo, 2022. The thesis author was a co-author of this paper.

ABSTRACT OF THE THESIS

Modeling Neurodevelopmental Ethanol Exposure

by

Justin Alan Truong

Master of Science in Biology

University of California San Diego, 2021

Professor Alysson Muotri, Chair
Professor Brenda Bloodgood, Co-chair

Prenatal alcohol exposure (PAE) is one of the leading preventable causes of neurodevelopmental disorders, underlying intellectual disability, cognitive dysfunction, and other neurocognitive symptoms associated with Fetal Alcohol Spectrum Disorder (FASD). Alcohol impacts diverse neural cell types; however, more specific pathophysiological effects on the human fetal cerebral cortex remain unclear. Here, we used human induced pluripotent stem cell (hiPSC)- derived cortical organoids and astrocytes, and primary human fetal neurons to explore cellular alterations induced by ethanol (EtOH) exposure. Within our human neural models, EtOH altered apoptosis, cell cycle, and proliferation. Additionally, expression of co-localized synaptic

puncta markers and synaptic proteins was reduced by early EtOH treatment. To potentially rescue these synaptic alterations, four drug compounds were employed; Donepezil, an acetylcholinesterase inhibitor commonly used to treat Alzheimer's symptoms and dementia, produced promising results for improving synaptic protein levels. Our study contributes to preliminary neurodevelopmental modeling of PAE- further defining cellular phenotypic signatures and elucidating potential therapeutic options.

INTRODUCTION

Despite public health efforts, prenatal alcohol exposure (PAE) remains the leading preventable cause of neurodevelopmental disorders, responsible for numerous defects found within Fetal Alcohol Spectrum Disorder (FASD)[1]. Alcohol use during pregnancy is directly linked to fetal alcohol syndrome (FAS), and despite underestimated FASD reports, global prevalence of alcohol consumption during pregnancy remains approximately 9.8%[2,3]. 1 in 67 pregnant women who consume alcohol are estimated to give birth to a child with FAS- translating to roughly 120,000 FAS newborns every year[3]. Furthermore, within the United States, FASDs together have a prevalence of approximately 2-5%[4,5]. FASD is diagnosed with a wide range of symptomatic severity, from neurobehavioral abnormalities to embryonic lethality. Intellectual disability, cognitive dysfunction, and behavioral deficits can underly secondary disabilities such as impaired learning, mental health issues, and addiction. Physical symptoms include microcephaly, abnormal cortical gyrification, growth deficiencies regarding weight and height, bone abnormalities, kidney and heart issues, as well as facial dysmorphisms[6–10].

Despite FASD public awareness, specific molecular pathophysiological and neurodevelopmental changes from EtOH exposure *in utero* remain understudied in humans. Previous *in vitro* and animal studies have identified a range of impact on neural functioning, with alterations dependent upon cell type and exposure severity[8,11–17]. However, suboptimal recapitulation of human cortical development in animal models has made clinically translating these results difficult[18]. Thus, human induced pluripotent stem cells (hiPSCs) provide an experimental platform for investigating EtOH-induced alterations in a dynamic neurodevelopmental context[19]. Moreover, hiPSCs can be aggregated and differentiated into 3D cortical organoids- resembling human fetal corticogenesis and serving not only a useful model to study mechanisms of neurodevelopmental disease, but also to screen potential therapeutic compounds in an ethical and cost-efficient manner[20–29].

Here, we found EtOH-induced, temporally specific changes in hiPSC-derived cortical organoids and astrocytes. Additionally, these alterations were validated by similar observations in primary fetal neurons. After generating and characterizing our human neural cellular models, we identified cellular phenotypic signatures that may influence broader FASD/PAE symptoms. Apoptosis, cell cycle, proliferation, and cortical organoid size are altered by EtOH exposure. Likewise, we saw reduced expression of synaptic markers and proteins in cortical organoids; using synaptic-related assays as readouts, we evaluated three cholinergic drugs (Donepezil, Nefiracetam, and PHA 543613) and one neurotrophic growth factor (IGF-1) to assess synaptic phenotypic rescue. Of these, Donepezil was able to ameliorate some EtOH-induced synaptic abnormalities. Altogether, our findings contribute to cortex-specific, neurodevelopmental disease modeling and promotes better understanding of early human brain vulnerability to environmental damage. Our platform provides a low-risk method for gaining insight into both PAE/FASD pathophysiology and therapeutic options.

MATERIALS AND METHODS

Human cell source (hiPSC and primary fetal tissue)

Three hiPSC lines, WT83C6 (male), CVB (male), and 4C1 (female) were derived from control skin fibroblast and dental pulp cells (DPCs); cells were reprogrammed, expanded, and previously validated elsewhere[29–31]. The hiPSC colonies were expanded on Matrigel-coated dishes (BD Biosciences, San Jose, CA, USA) using either mTeSR1 or mTeSR Plus medium (StemCell Technologies, Vancouver, Canada). The cells were regularly karyotyped and underwent CNV arrays to avoid genomic alterations in the culture. Embryonic samples were obtained from fetal brains (10-11 weeks post-conception (PCW)) and cultured in Neurobasal (Life Technologies, Carlsbad, CA, USA) supplemented with 1X GlutaMAX (Life Technologies), 1% Gem21 NeuroPlex (Gemini Bio-Products, West Sacramento, CA, USA), 1% MEM nonessential amino acids (NEAA; Life Technologies), and 1% penicillin/streptomycin (Pen/Strep; Life Technologies). PCR mycoplasma testing was routinely performed. The study was approved by the University of California San Diego IRB/ESCRO committee (protocol 141223ZF).

Generation of Cortical Organoids

HiPSCs were dissociated using Accutase (Life Technologies) and PBS for 10 minutes (37 °C) and centrifuged (150 *x g*, 3 minutes). Cells were resuspended in mTeSR1 including 10 µM SB431542 (SB; Stemgent, Cambridge, MA, USA), 1 µM Dorsomorphin (Dorso; R&D Systems, Minneapolis, MN, USA), and 5 µM ROCK inhibitor (for first 24hrs, Y-27632; Calbiochem, Sigma-Aldrich, St. Louis, MO, USA). Approximately $4x10^6$ cells were seeded to each well of 6-well plates and kept in suspension under rotation (95 rpm) for 3 days. Then, for 24 days, the cell aggregates were maintained in defined culture media cycling through factors promoting proliferation, maturation, gliogenesis, and activity. Media1 [Neurobasal (Life

Technologies) supplemented with GlutaMAX, 1% Gem21 NeuroPlex (Gemini Bio-Products), 1% N2 NeuroPlex (Gemini Bio-Products), 1% NEAA (Life Technologies), 1% PS (Life Technologies), 10 µM SB and 1 µM Dorso] for 6 days. Media2 [Neurobasal with GlutaMAX, 1% Gem21 NeuroPlex, 1% NEAA and 1% PS] supplemented with 20 ng/mL FGF2 (Life Technologies) for one week. Media2 including 20 ng/mL EGF and FGF (PeproTech, Rocky Hill, NJ, USA) for 6 days. Media3 [Media2 supplemented with 10 ng/mL of BDNF, 10 ng/mL of GDNF, 10 ng/mL of NT-3 (PeproTech), 200 µM L-ascorbic acid and 1 mM dibutyryl-cAMP (Sigma-Aldrich)] for 6 days. Cortical organoids were maintained beyond 24 days in Neurobasal supplemented with GlutaMAX, 1% Gem21 NeuroPlex, 1% NEAA, 1% Pen/Strep with media changes 3-4 times per week.

Generation of astrocytes

Neural progenitor cells were dissociated with PAPAIN, DNase 1, and EBSS (Worthington Biochemical Corporation, Lakewood, NJ, USA, 37 °C, 15 minutes). Roughly $5x10^6$ cells per well were seeded in neural media [DMEM/F12 (Life Technologies) supplemented with 1X GlutaMAX, 1X Gem21 (Gemini Bio-products), and 1X Pen/Strep (Life Technologies)] containing 20 ng/mL FGF2 (PeproTech). 6 well plates were kept in suspension under rotation. ROCK inhibitor (Y-27632; Calbiochem, Sigma-Aldrich, St. Louis, MO, USA) was added to a final concentration of 5 µM for 48 hours. After the removal of ROCK inhibitor, neural media without bFGF was used for one week. Next, astrocyte growth media (Lonza Group, Basel, Switzerland) was used for two weeks until plated onto dishes pre-coated with 100 µg/mL poly-L-ornithine and 10 µg/mL laminin. The spheres were further cultured in AGM as astrocytes projected outward to populate the plate.

Alcohol (EtOH) exposure strategy

Cortical organoids (around 1 month-old), hiPSC-derived astrocytes, and primary fetal neurons were exposed to EtOH by supplementing the culture media with 200-proof EtOH (100mM, Sigma-Aldrich) for seven days, with media changes every other day. After this period, cells were maintained in media without EtOH for as long as specified in each experiment. Although initial exposure was 100 mM EtOH, the final EtOH concentration in the media stabilized around 20 mM after a couple of hours, as demonstrated by measurements over time using the DensitoPro Handheld Density Meter (Mettler Toledo, Columbus, OH, USA, Figure 1D). Cells were incubated at 37 °C throughout treatment. To maintain a stable environmental concentration close to 20 mM and avoid evaporation of EtOH, cells were always cultured in an EtOH-saturated atmosphere. Control untreated and treated cells were kept separate and covered to avoid cross-contamination and EtOH leakage.

Immunofluorescence staining

Cells were fixed with 4% paraformaldehyde, permeabilized and blocked with 0.1% Triton X-100 and 3% FBS in PBS, and incubated with primary antibodies overnight at 4 ºC. Primary antibodies used were: rat anti-CTIP2, ab18465 (Abcam, Cambridge, United Kingdom), 1:500; rabbit anti-cleaved-caspase-3, #9661 (Cell Signaling, Danvers, MA, USA), 1:400; chicken anti-MAP2, ab5392 (Abcam), 1:2000; mouse anti-NeuN, MAB377 (EMD-Millipore, Burlington, MA, USA), 1:500; rabbit anti-Ki67, ab15580 (Abcam), 1:1000; rabbit anti-GFAP, Z033429 (DAKO A/S, Glostrup, Denmark), 1:1000; mouse anti-Vglut1, 135311 (Synaptic Systems, Goettingen, Germany), 1:500; rabbit anti-Homer1, 160003 (Synaptic Systems), 1:500. After being washed with PBS, samples were incubated with secondary antibodies (Alexa Fluor 488-, 555- and 647-conjugated antibodies, Life Technologies, 1:1000) for two hours at room temperature. The slides were mounted using ProLong Gold antifade reagent (Thermo Fisher Scientific, Waltham, MA, USA) and analyzed under an Apotome fluorescence microscope.

Cell cycle analysis

Cortical organoids, primary fetal neurons, and astrocytes were manually dissociated and counted using a Via1-Cassette with the NucleoCounter NC-3000 (Chemometec, Allerod, Denmark). First, dissociated cells were fixed with 70% EtOH for two hours. Next, the cells were resuspended in 0.5 µg/ml DAPI, 0.1% Triton X-100 in PBS, and incubated at 37 ºC for five minutes. Finally, cells were loaded into an NC-Slide A2 chamber (Chemometec), and cellular fluorescence was quantified with the NucleoCounter NC-3000 using the manufacturer's protocol.

Annexin and cell death

Primary fetal neurons and astrocytes were manually dissociated and resuspended in Annexin V binding buffer (Invitrogen). Next, Annexin V-CF488A conjugate (Biotium, Inc., Hayward, CA, USA) was added, followed by Hoechst 33342 (Chemometec). After a PBS wash, the cells were resuspended in Annexin V binding buffer (Invitrogen) containing 10 µg/mL propidium iodide (Chemometec). Cells were loaded into NC-Slide A2 chambers, and the "Annexin V Assay" was run with the NucleoCounter NC-3000.

Synaptic puncta quantification

Co-localized pre (Vglut1+) and postsynaptic (PSD95+) puncta were quantified along MAP2+ neuronal processes using reconstructed three-dimensional z-stack images of neurons from control, EtOH treated, and drug treated cortical organoids. The primary antibodies (Vglut1, 1:1000, Synaptic Systems; PSD95, 1:1000, NeuroMab; and MAP-2, 1:2000, Sigma-Aldrich) were incubated for two hours at room temperature. After wash, secondary antibodies (Alexa Fluor 488-, 555- and 647-conjugated antibodies, 1:1000, Life Technologies) were incubated for one hour. Coverslips were mounted, and slides were analyzed (puncta were counted) under a fluorescence microscope (Z1 Axio Observer Apotome, Zeiss).

Cortical organoid dissociation

Cortical organoids from each treatment condition were harvested and washed with PBS. Spheres were dissociated by incubation (37 ºC) under rotation in Accumax (StemCell Technologies, Vancouver, Canada) for 20 minutes, gently pipetted, and then incubated for an additional 10 minutes. Neurobasal supplemented with GlutaMAX, 1% Gem21 NeuroPlex, 1% NEAA, and 1% Pen/Strep was used to neutralize Accumax while gently pipetting. Samples were centrifuged (200 x g, 4min), resuspended in Neurobasal, and seeded onto chamber slides (Thermo Fisher Scientific, density based on manufacturer specifications, Nunc™ Lab-Tek™ II 4 and 8 well systems). The NucleoCounter NC-3000 was used to assess cell viability and density. To permit neuronal outgrowth and reconnection, cells were cultured for 1 week prior to puncta staining.

Western blotting

Cortical organoid protein from each treatment was collected using RIPA Lysis and Extraction buffer (ThermoScientific) with PhosSTOP phosphatase inhibitor (Roche) and cOmplete ULTRA mini protease inhibitor (Roche). Total protein was extracted and quantified with the BCA Protein Assay Kit (Pierce Biotechnology, Rockford, IL, USA). 20µg of protein was separated on a 4–12% Bis-Tris protein gel (Novex), transferred using the iBlot2 Gel Transfer device (ThermoScientific) onto a nitrocellulose membrane (Novex) gel, blocked with Rockland Blocking Buffer (Rockland, 4°C, gently shaking, 4hrs), and incubated overnight at 4°C with primary antibodies. Antibodies used: rabbit anti-Synapsin1, AB1543P, (EMD-Millipore), 1:1000; mouse anti-PSD95 NeuroMab, 1:1000; mouse anti-β-Actin, ab8226 (Abcam), 1:5000); followed by two-hour incubation with secondary antibodies (Li-Cor 680-, 800-, 1:5000) before imaging and quantification using the Odyssey CLx imaging system (Li-Cor, Lincoln, NE, USA).

Drug Treatments

Donepezil, Nefiracetam, PHA-543,613, (Tocris, Minneapolis, MN, USA) and IGF-1 (Peprotech) were prepared according to manufacturer specifications; compounds were diluted to a working stock of 1mM. 2.5-month-old cortical organoids (EtOH exposed for 1 week at ~1 month old) were drug treated for 3 weeks (1uM) before harvest and assays. EtOH controls received corresponding volumes of DMSO (<0.01%) or DI water vehicle. Compounds were supplemented in media changes 3 times per week.

Statistical analysis

Statistical analysis was performed using GraphPad Prism versions 8 and 9 (GraphPad Software, La Jolla, CA, USA). Results from continuous variables are presented as mean ± standard error of the mean (s.e.m.), and 95% confidence intervals were normal-based. Means were compared between groups using, where appropriate, unpaired Student's *t*-test, one-way, or two-way analyses of variance (ANOVA). Whenever possible, the investigator was blind to the sample conditions. Tests were performed two-sided with α throughout set as 0.05.

RESULTS

Human cellular models express neural markers and resemble early corticogenesis

Human cell platforms were used to investigate neurodevelopmental alterations from EtOH exposure. Immunohistochemistry in cortical organoids displayed similar cytostructural complexity and temporal development to that of fetal corticogenesis. Diverse cell types for both control and EtOH-exposed cortical organoids (EtOH-treated around 1 month-old) organized into regions surrounding varying lumens. Innermost layers resembled the ventricular zone (VZ, SOX2+ progenitors enriched for proliferation marker Ki67+) underlying a sub-ventricular zone (SVZ containing intermediate progenitors); expanding outward, cell types resembling a cortical plate expressed mature neurons (NeuN+, MAP2+) with deep-cortical layer specificity (CTIP2+, Figure 1A,B). Primary fetal neurons likewise expressed deep-cortical markers (CTIP2+, MAP2+) and help validate our EtOH-induced neurodevelopmental findings in hiPSC-derived models. To capture more neural cell types, astrocytes were generated separately and expressed glial marker GFAP+ (Figure 1A). Notably, glial expression emerges later in neurodevelopment and is thus scarce in early cortical organoids[24].

Each cell culture received moderate-high (100mM) physiological concentration EtOH for one week followed by maintenance in the absence of EtOH. Although 100mM EtOH exposure is high, the actual concentration cells were kept corresponds to ~20mM or 92 mg/dL (3-5 average drinks, Figure 1D). A handheld density meter was used to record EtOH concentration over time in media at 37°C; results showed EtOH decay and stabilization to ~20mM within two hours (Figure 1D). This treatment dosage was selected considering EtOH cytotoxicity and its concentration in amniotic fluid[32–35].

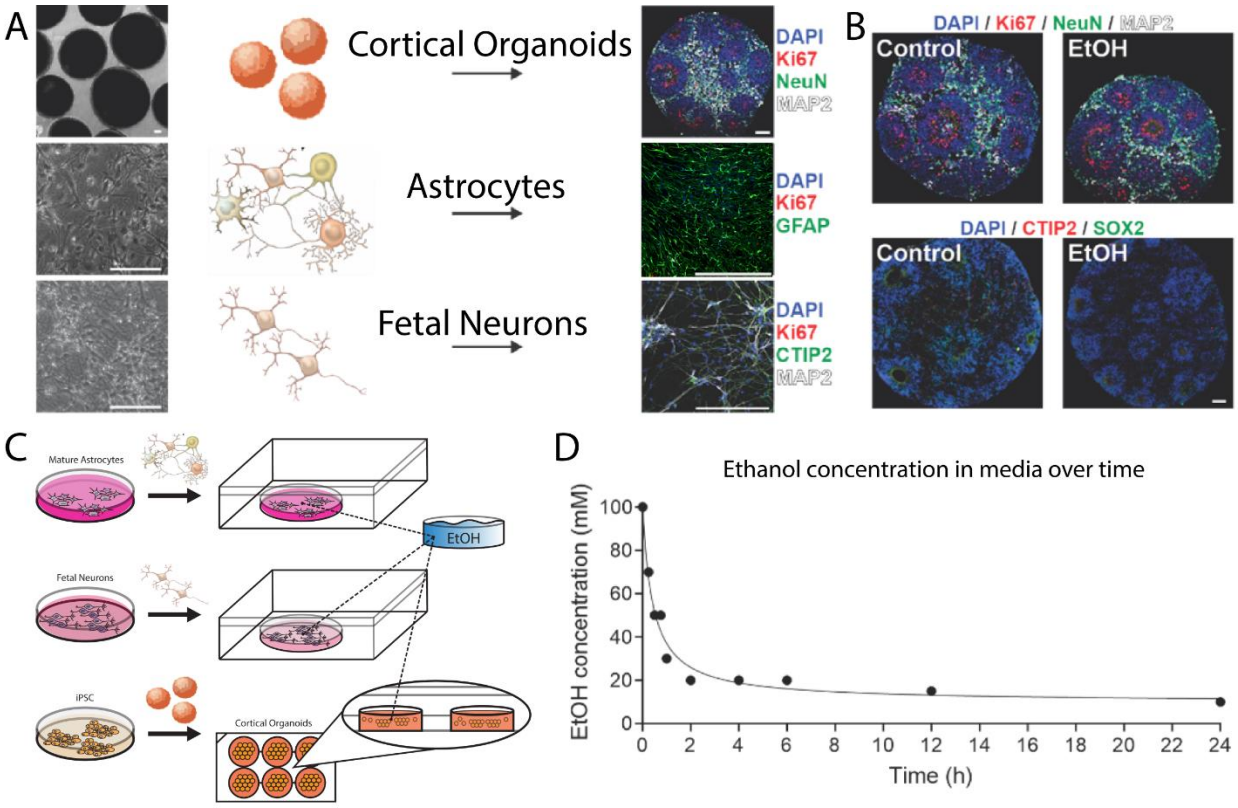

Figure 1: Characterization of human cellular models and alcohol exposure strategy. **A.** Human iPSC-derived cortical organoids (COs), iPSC-derived astrocytes, and primary fetal neurons were generated or cultured. Immunohistochemistry showed proliferative (Ki67+), mature neuronal (NeuN+, MAP2+), deep cortical layer (CTIP2+), and glial (GFAP+) markers. **B.** IHC in cortical organoids portrayed neural stem and progenitor (SOX2+), proliferative (Ki67+), mature neuronal (NeuN+, MAP2+), and deep cortical (CTIP2+) markers. **C.** EtOH exposure scheme showing containment method to promote EtOH-saturated environments. **D.** EtOH concentration in media decreased within two hours and stabilized around 20mM over time.

EtOH exposure alters apoptosis, cell cycle, and proliferation

To determine whether EtOH leads to cell death and alterations in cell cycle/proliferation, we used annexin, cell cycle, and Ki67 staining assays. Unsurprisingly, EtOH exposure increased early apoptosis in astrocytes and primary fetal neurons- assessed by Annexin+ cell frequency ($P < 0.05$; Figure 2A,B,D). Along a range of concentrations, significant astrocytic cell death was initially seen at 100mM EtOH treatment (Figure 2B). Likewise, we observed more apoptotic cells (Cleaved Caspase 3, CC3+) in two-month-old EtOH-exposed organoids compared to controls (P

< 0.05; Figure 2C). Cell cycle analysis revealed EtOH-induced alteration in cortical organoids, astrocytes, and fetal neurons; cell types were less likely to be in the proliferative S and G2/mitotic phases (P < 0.05 for cortical organoids; 2E,F,G). However, fetal neurons and astrocytes had more subtle alterations most likely due to cell type maturity. To further assess proliferative changes in organoids, we observed a smaller population of Ki67+ (proliferation marker) cells in EtOH-exposed cultures (*P* < 0.0001, Figure 1H); ensuring comparable organoid sections, the overall quantity of DAPI+ cells remained constant- independent of treatment. Additionally, EtOH exposure reduced cortical organoid diameter, possibly due to cell apoptotic/proliferative alteration, at two-months-old compared to controls (*P* < 0.0001; Figure 2I).

Figure 2: EtOH exposure alters apoptotic and cell cycle profiles in human neural models. **A, B.** EtOH induced cell death in astrocytes (shown by Annexin+ scatterplots). Range of EtOH doses portrayed initial threshold (100mM) for significant cell death (one-way analysis of variance (ANOVA), $F_{6,7} = 53.0252$, P<0.0001; post-hoc Tukey HSD Test, Control vs. 100mM: Q statistic = 5.8148, P<0.05; n=4 replicates/condition). **C, D.** EtOH induced cell death in two-month-old cortical organoids and fetal neurons, shown by cleaved caspase-3+ IHC (Student's *t*-test, $t_{28} = 5.785$, $P<0.0001$; n=10-15 organoids/condition) and Annexin+ staining (Student's *t*-test, $t_6 = 7.872$, $P=0.0002$; n=4 replicates/condition), respectively. **E-G.** EtOH exposure altered cell cycle profiles in astrocytes (two-way ANOVA, $F_{2,42} = 17.06$, $P<0.0001$), cortical organoids (two-way ANOVA, $F_{3,16} = 8.14$, $P=0.002$), and fetal neurons (two-way ANOVA, $F_{2,42} = 41.92$, $P<0.0001$), respectively. **H.** Across multiple layers, immunohistochemistry in EtOH-cortical organoids revealed differential Ki67+ expression compared to controls (two months, Student's *t*-test, $t_{64} = 4.518$, $P<0.0001$; n=10-33 organoids/condition). **I.** Cortical organoid diameter is decreased by EtOH exposure (Student's *t*-test, $t_{541} = 17.05$, $P<0.0001$; n=210-333 organoids/condition).

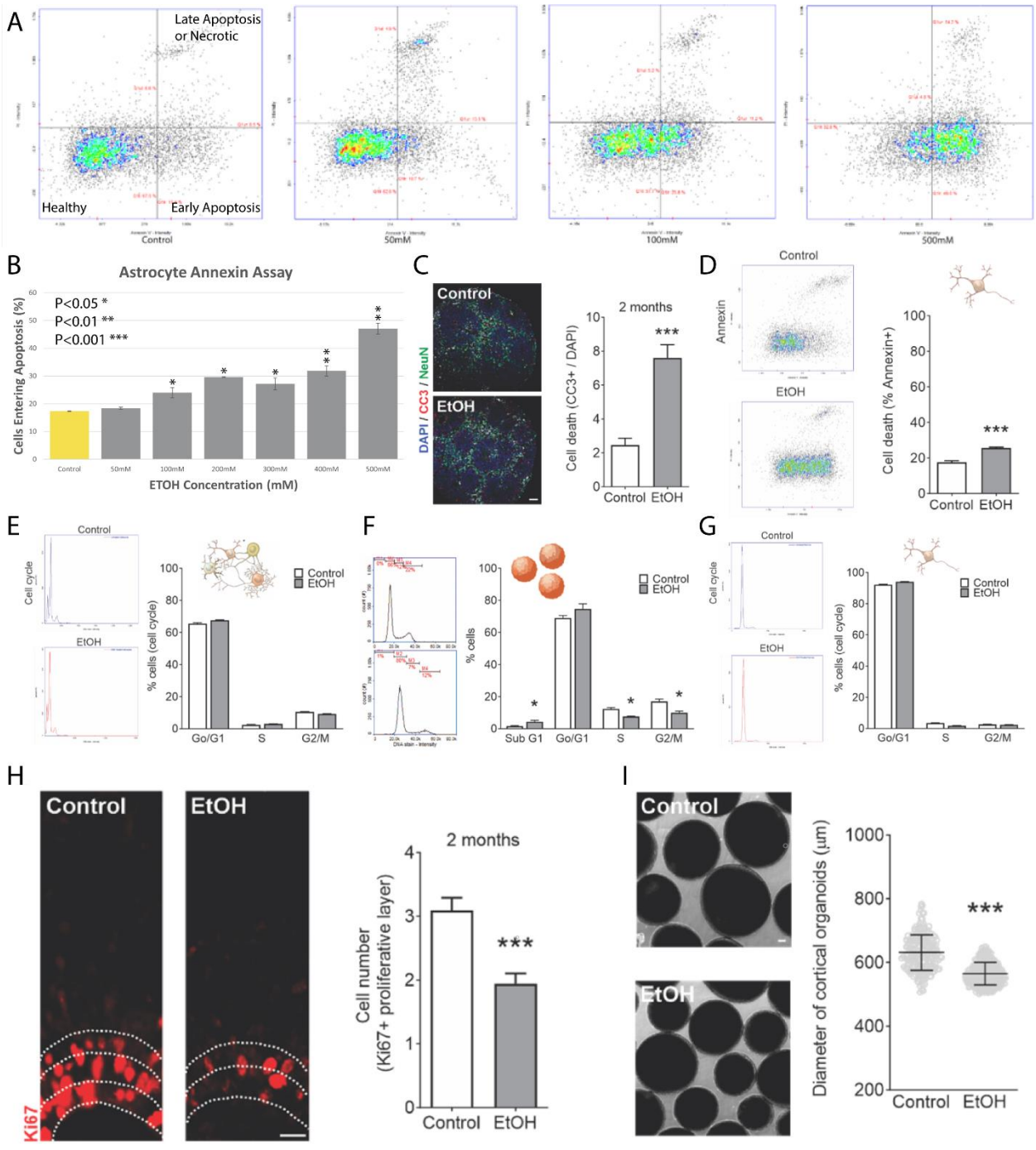
A
Late Apoptosis or Necrotic
Healthy
Early Apoptosis
Control
50mM
100mM
500mM
B
Astrocyte Annexin Assay
P<0.05 *
P<0.01 **
P<0.001 ***
Cells Entering Apoptosis (%)
Control
50mM
100mM
200mM
300mM
400mM
500mM
ETOH Concentration (mM)
C
Control
EtOH
DAPI / CC3 / NeuN
2 months
Cell death (CC3+ / DAPI)
Control EtOH
D
Control
EtOH
Annexin
Cell death (% Annexin+)
Control EtOH
E
Control
EtOH
Cell cycle
% cells (cell cycle)
Control
EtOH
Go/G1
S
G2/M
F
% cells
Control
EtOH
Sub G1
Go/G1
S
G2/M
G
Control
EtOH
Cell cycle
% cells (cell cycle)
Control
EtOH
Go/G1
S
G2/M
H
Control
EtOH
Ki67
2 months
Cell number (Ki67+ proliferative layer)
Control EtOH
I
Control
EtOH
Diameter of cortical organoids (µm)
Control EtOH

Rescue of altered synaptic markers in neurons from EtOH-exposed cortical organoids

After identifying EtOH-induced impairment of synaptic markers, four drug compounds were tested for phenotypic rescue, using synaptic puncta staining and western blot analysis as readouts. Donepezil treatment in EtOH-exposed cortical organoids increased expression of co-localized synaptic puncta density; similarly, Donepezil treatment rescued pre (SYN1) and post synaptic (PSD95) protein expression (Figure 3A,B,C). PHA-543,613 likewise increased both pre and post synaptic protein expression (Figure 3F). Surprisingly, Nefiracetam and IGF-1 had mixed results. Nefiracetam appeared to rescue co-localized synaptic puncta density but did not reach statistical significance (P=0.1109); western blots revealed rescue of PSD95 expression, and yet reduced SYN1 expression compared to EtOH-exposed organoids (Figure 3A,B,D). IGF-1 had little effect on synaptic protein expression, with slight PSD95 increase and subtle SYN1 decrease (Figure 3E).

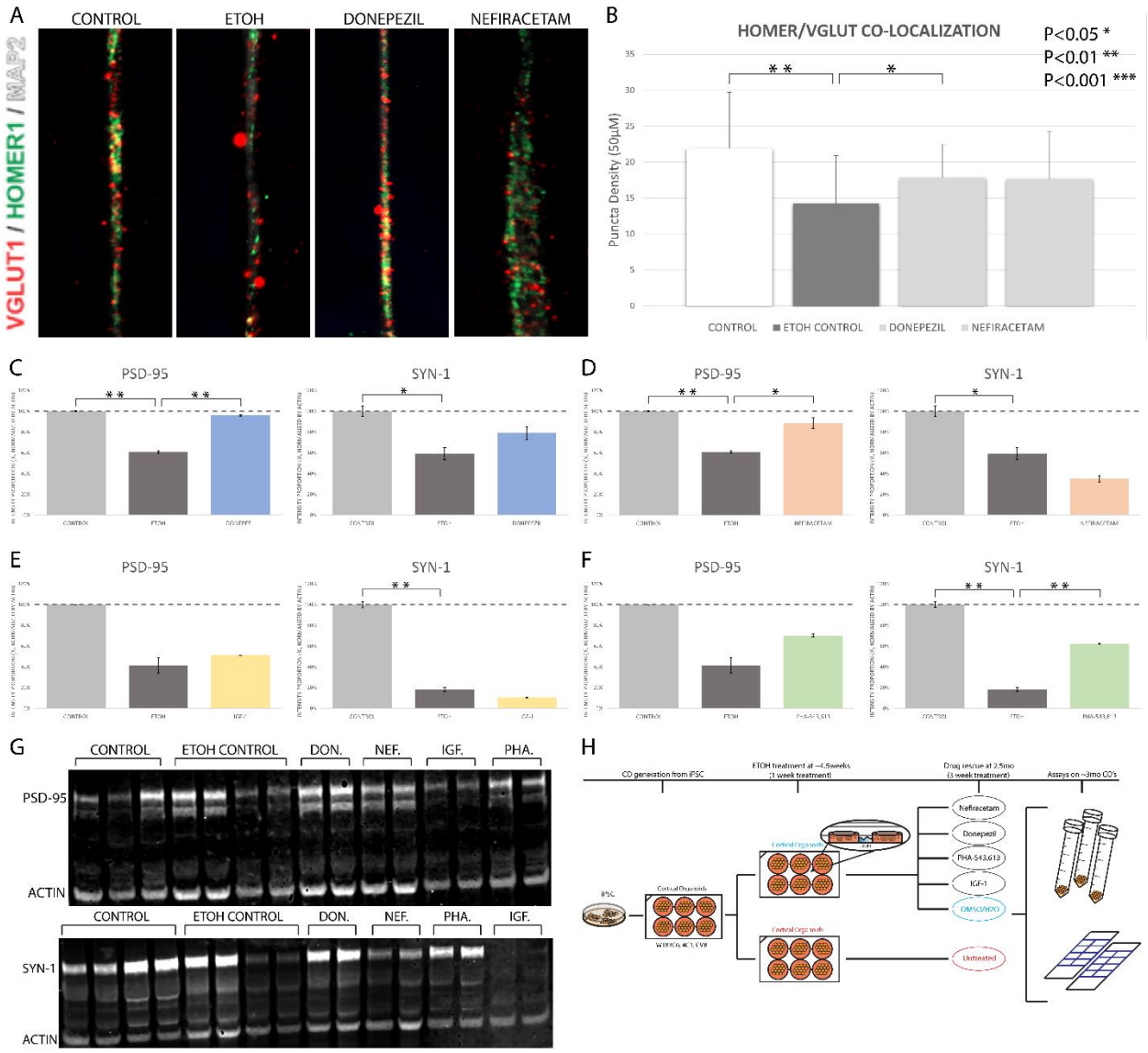

Figure 3: Drug treatments impact synaptic protein expression and puncta density co-localization in EtOH-impaired cortical organoids.
A, B. Donepezil rescued EtOH-decrease of co-localized synaptic puncta density (one-way ANOVA, $F_{3,173} = 10.8595$, $P<0.0001$; post-hoc Tukey HSD Test, Control vs. EtOH: Q statistic = 8.0552, $P<0.01$; EtOH vs. Donepezil Rescue: Q statistic = 4.0706, $P<0.05$; EtOH vs. Nefiracetam Rescue: Q statistic = 3.2006, $P>0.05$; n=12 neurons/condition from 3mo COs). **C, D, E, F.** Donepezil, Nefiracetam, IGF-1, and PHA-543,613, respectively, on EtOH-impaired COs increased synaptic protein expression in some cases (one-way ANOVA for each drug condition in either protein, converted to proportions of 100% untreated control, Donepezil PSD95 and SYN1: $F_{2,3} = 726.1663$ and $F_{2,3} = 13.1481$, $P<0.0001$ and $P<0.05$; Nefiracetam PSD95 and SYN1: $F_{2,3} = 41.4344$ and $F_{2,3} = 47.5267$, $P<0.01$ and $P<0.01$; IGF1 SYN1: $F_{2,3} = 595.5744$, $P<0.001$; PHA-543,613 SYN1: $F_{2,3} = 400.2451$, $P<0.001$). IGF-1 and Nefiracetam treatments did not increase EtOH-impaired expression of pre-synaptic protein (SYN-1). **G.** Synaptic protein WB bands of all conditions. **H.** Scheme outlining cortical organoid EtOH exposure and drug treatment timeline.

The Introduction, Material and Methods, and Results section with corresponding figures, in part, contain or are inspired by manuscript components submitted for publication; the material may appear in Life Science Alliance, 2022, Jason W. Adams, Priscilla D. Negraes, Justin Truong, Timothy Tran, Ryan Szeto, Carmen Teodorof, Stephen A. Spector, Miguel Del Campo, Kenneth L. Jones, Alysson R. Muotri and Cleber A. Trujillo, 2022. The thesis author was a co-author of this paper.

DISCUSSION

Linking our EtOH-induced cellular changes to PAE/FASD symptoms

In this present study, we utilized iPSC-derived cortical organoids, iPSC-derived astrocytes, and primary fetal neurons to assess temporally specific, EtOH-induced changes in cell and protein dynamics. Modeling neurodevelopmental alcohol exposure, our findings concerning altered apoptosis, cell cycle, proliferation, and synaptic markers may underpin broader symptoms characteristic of FASD. More specifically, these neurodevelopmental changes are likely associated to neurodegeneration underlying behavioral and physiological abnormalities. EtOH-induced neurodegeneration, linked to higher cell death, altered cell cycle profiles, and hindered proliferation, is associated with consequences in neural circuit dysfunction, neural/synaptic plasticity, and synaptic transmission[36–41]. Additionally, studies suggest EtOH-induced, apoptotic neurodegeneration yielding neurotoxicity by detrimental proinflammatory responses following astrocytic activation[42].

Our identified neurodevelopmental effects, acute cellular abnormalities associated to neurodegeneration, may manifest as the FASD behavioral and physiological signs we commonly observe. Deficits in cognition, memory, and learning for instance or greater predisposition to neurological diseases, spanning Alzheimer's, Frontotemporal Dementia, Schizophrenia, and

Parkinson's[38,40,43–46]. Similarly, the culmination of these neurodevelopmental cellular defects likely fosters physical malformations of microcephaly, abnormal cortical gyrification, and impaired growth and weight[9,47–49]. Agreeing with our observations of reduced cortical organoid size, magnetic resonance imaging (MRI) in FASD patients portrays volumetric reductions in the cortex, corpus callosum, cerebellum, and other subcortical structures[54-57]. Additionally, the fewer dividing cells during proliferative stages and increased cell death in our cortical organoids aligns with reported phenotypes of other model systems[58,59].

The cholinergic system and drug treatment rationale

Given the importance of cholinergic transmission throughout the central nervous system, affecting memory, learning, and higher order thinking, combined with lacking approved pharmacological interventions for FASD, we explored primarily cholinergic acting compounds[50]. Choline supplementation, both pre and postnatally, within animal models has been shown to improve FASD symptoms, including low birth weight and cognitive impairment; FASD children receiving choline therapy also exhibit minimal adverse effects- underscoring the potential for cholinergic targeting toward improving FASD neurodevelopmental dysfunction[51].

Donepezil, an acetylcholinesterase inhibitor, is used for ameliorating cognitive/intellectual deficits in Rett syndrome and Alzheimer's- reducing synaptic acetylcholine depletion and improving cholinergic transmission[52,53]. Nefiracetam, a cholinergic, GABAergic, and glutamatergic agonist, targets neuronal nicotinic acetylcholine receptors (nnAChRs) to rescue synaptic dysfunction and enhance cognition; the neuroprotective compound has been used in Alzheimer's, Rett syndrome (RTT), and post-stroke dementia studies[27,54]. Likewise, agonist PHA-543,613 targets nnAChRs (α7)- improving synaptic morphology, synaptic function, and neuronal network activity in neurodevelopmental disease models; the neuroprotective agent combats pathophysiology in MECP2 deficiency studies (RTT) and is implicated in treating

schizophrenia[54,55]. IGF-1, which promotes neuronal proliferation and survival, is less specific in therapeutic targeting due to ubiquitous expression- driving growth and differentiation of numerous cell types[56]. Additionally, the controversial neurotrophic factor yields fluctuating effects on neuroinflammatory regulation and has context-dependent pro-epileptic and neurotoxic capabilities[57,58]. The context-sensitive nature and necessary fine regulation may contribute to our absence of distinct rescue. Nevertheless, IGF-1 benefit is demonstrated in model systems and has shown promise in clinical autism research[59].

Drug therapy takeaway

Of the four treatments, Donepezil showed the most potential- rescuing synaptic puncta co-localization and increasing both pre and post synaptic protein expression. Acetylcholinesterase inhibition promotes cholinergic transmission and associated neurobehavioral health; given acetylcholine's neuromodulator role in synaptic plasticity and transmission, our results support Donepezil's therapeutic potential for FASD symptoms via cholinergic and synaptic pathways[53,60,61]. Similarly, our rescue agrees with Donepezil reports regarding treatment for synaptic loss and neurodegeneration in tau pathology[62]. Human neuroblastoma studies also implicate Donepezil-attenuation of EtOH-induced apoptosis, toxicity, and cognitive harm[63]. Further testing the relationship between Donepezil and EtOH-induced apoptosis in cortical organoids, supplemented with electro-functional and synaptic readouts, would be interesting toward assessing drug mediated toxicity and functionality within our model.

FASD and PAE have been associated to increased risk of other neurodegenerative diseases; thus, testing Donepezil, Nefiracetam, PHA-543,613, and IGF-1, drugs commonly used in therapeutic treatments/studies regarding neurodegeneration and neuroprotection, allowed FASD pathophysiological discovery and rescue with supporting context of diseases containing related pathological mechanisms[27,54,55,57,59,62–64]. It would be interesting to further explore molecular and

cellular overlap behind neurodegeneration across differing disorders; elucidating conserved targets could benefit therapeutic progress in terms of prevention and cost.

Limitations and expanding our research

Although this study is a step towards understanding PAE, it has several intrinsic limitations. Despite technological advancements, cortical organoids and astrocytes are only cellular models rather than genuine human brains, so making a direct judgment about the full effects of *in utero* EtOH exposure remains elusive. We have sought to minimize this limitation by including human primary fetal neurons, which appear to validate the findings in the cortical organoids. Another barrier is that EtOH concentration and exposure are unavoidably different from those experienced during fetal development, particularly considering fetal recycling of amniotic fluid and the consequent risk of prolonged EtOH exposure *in utero*[76]. Third, the drugs were administered during early neurodevelopmental periods to target even earlier EtOH insults; the maturity within our models is difficult to translate clinically[27]. Thus, expanding the study length and optimizing a high throughput platform will be necessary toward achieving physiological relevance- especially considering the temporal complexity and varying symptom severity within PAE[65]. Increasing cortical organoid age will also help capture an astrocytic population within a PAE setting- valuable toward more accurate human neural modeling as well as investigating ETOH-induced alterations in relation to glia[66,67]. Furthermore, diverging conclusions within our study, regarding Nefiracetam and IGF-1 synaptic protein rescue, require additional investigation. Likewise, dose curve experiments and tracking cytotoxicity to fine tune therapeutic options is the next logical step in improving our impact.

Although unlikely that these acute neurotoxic mechanisms solely influence neurodegeneration and subsequent physiological and behavioral diagnoses, identifying these alterations, in tandem with drug screening, provides a more comprehensive understanding of

PAE/FASD. This study conveys preliminary steps toward advancing neurodevelopmental models of EtOH exposure and bettering FASD neuropathology.

APPENDIX

Supplementary Table 1: Overall Western Blot Tukey HSD Results

Overall Tukey HSD results for each western blot plot/data set across synaptic proteins and drug treatments. Note absence of ANOVA statistical testing for PSD-95 sets: IGF-1 and PHA-543,613; western blot gel was lacking an untreated control replicate lane, thus, ANOVA statistical testing on dataset containing a condition without enough values was invalid (P<0.05*, P<0.01**, P<0.001***).

Tukey HSD results Western Blots									
PSD-95 DONEPEZIL				SYN-1 DONEPEZIL					
treatments	Tukey HSI	Tukey HSI	Tukey HSD	treatments	Tukey HSI	Tukey HSI	Tukey HSD		
pair	Q statistic	p-value	inferfence	pair	Q statistic	p-value	inferfence		
CTR Vs. ETOH	49.0103	0.001005	** p<0.01	CTR Vs. ETOH	7.2503	0.028977	* p<0.05		
CTR Vs Done.	5.0888	0.072816	insignificant	CTR Vs. Done.	3.7644	0.146893	insignificant		
ETOH Vs. Done.	43.9215	0.001005	** p<0.01	ETOH Vs. Done.	3.4859	0.17284	insignificant		
PSD-95 NEFIRACETAM				SYN-1 NEFIRACETAM					
treatments	Tukey HSI	Tukey HSI	Tukey HSD	treatments	Tukey HSI	Tukey HSI	Tukey HSD		
pair	Q statistic	p-value	inferfence	pair	Q statistic	p-value	inferfence		
CTR Vs ETOH	12.5119	0.006219	** p<0.01	CTR Vs ETOH	8.5491	0.018386	* p<0.05		
CTR Vs. NEF.	3.6307	0.158718	insignificant	CTR Vs. Nef.	13.6428	0.004838	** p<0.01		
ETOH Vs. Nef	8.8812	0.016527	* p<0.05	ETOH Vs. Nef.	5.0937	0.072645	insignificant		
PSD-95 IGF-1	NA	NA	NA	SYN-1 IGF-1					
				treatments	Tukey HSI	Tukey HSI	Tukey HSD		
				pair	Q statistic	p-value	inferfence		
				CTR Vs. ETOH	40.3123	0.001005	** p<0.01		
				CTR Vs. IGF-1	43.987	0.001005	** p<0.01		
				ETOH Vs. IGF-1	3.6747	0.154708	insignificant		
PSD-95 PHA-543,613	NA	NA	NA	SYN-1 PHA-543,613					
				treatments	Tukey HSI	Tukey HSI	Tukey HSD		
				pair	Q statistic	p-value	inferfence		
				CTR Vs. ETOH	39.9714	0.001005	** p<0.01		
				CTR Vs. PHA.	18.42	0.002006	** p<0.01		
				ETOH Vs. PHA.	21.5514	0.00126	** p<0.01		

REFERENCES

1. Roozen, S., Peters, G.-J. Y., Kok, G., Townend, D., Nijhuis, J., & Curfs, L. (2016). Worldwide Prevalence of Fetal Alcohol Spectrum Disorders: A Systematic Literature Review Including Meta-Analysis. *Alcoholism: Clinical and Experimental Research*, *40*(1). https://doi.org/10.1111/acer.12939

2. Popova, S., Lange, S., Probst, C., Gmel, G., & Rehm, J. (2017). Estimation of national, regional, and global prevalence of alcohol use during pregnancy and fetal alcohol syndrome: a systematic review and meta-analysis. *The Lancet Global Health*, *5*(3). https://doi.org/10.1016/S2214-109X(17)30021-9

3. May, P. A., Baete, A., Russo, J., Elliott, A. J., Blankenship, J., Kalberg, W. O., Buckley, D., Brooks, M., Hasken, J., Abdul-Rahman, O., Adam, M. P., Robinson, L. K., Manning, M., & Hoyme, H. E. (2014). Prevalence and Characteristics of Fetal Alcohol Spectrum Disorders. *PEDIATRICS*, *134*(5). https://doi.org/10.1542/peds.2013-3319

4. May, P. A., Chambers, C. D., Kalberg, W. O., Zellner, J., Feldman, H., Buckley, D., Kopald, D., Hasken, J. M., Xu, R., Honerkamp-Smith, G., Taras, H., Manning, M. A., Robinson, L. K., Adam, M. P., Abdul-Rahman, O., Vaux, K., Jewett, T., Elliott, A. J., Kable, J. A., … Hoyme, H. E. (2018). Prevalence of Fetal Alcohol Spectrum Disorders in 4 US Communities. *JAMA*, *319*(5). https://doi.org/10.1001/jama.2017.21896

5. May, P. A., Gossage, J. P., Kalberg, W. O., Robinson, L. K., Buckley, D., Manning, M., & Hoyme, H. E. (2009). Prevalence and epidemiologic characteristics of FASD from various research methods with an emphasis on recent in-school studies. *Developmental Disabilities Research Reviews*, *15*(3). https://doi.org/10.1002/ddrr.68

6. Jones, KennethL., & Smith, DavidW. (1973). RECOGNITION OF THE FETAL ALCOHOL SYNDROME IN EARLY INFANCY. *The Lancet*, *302*(7836). https://doi.org/10.1016/S0140-6736(73)91092-1

7. Hoyme, H. E., Kalberg, W. O., Elliott, A. J., Blankenship, J., Buckley, D., Marais, A.-S., Manning, M. A., Robinson, L. K., Adam, M. P., Abdul-Rahman, O., Jewett, T., Coles, C. D., Chambers, C., Jones, K. L., Adnams, C. M., Shah, P. E., Riley, E. P., Charness, M. E., Warren, K. R., & May, P. A. (2016). Updated Clinical Guidelines for Diagnosing Fetal Alcohol Spectrum Disorders. *Pediatrics*, *138*(2). https://doi.org/10.1542/peds.2015-4256

8. Rasmussen, C., Andrew, G., Zwaigenbaum, L., & Tough, S. (2008). Neurobehavioural outcomes of children with fetal alcohol spectrum disorders: A Canadian perspective. *Paediatrics & Child Health*, *13*(3).

9. Hendrickson, T. J., Mueller, B. A., Sowell, E. R., Mattson, S. N., Coles, C. D., Kable, J. A., Jones, K. L., Boys, C. J., Lim, K. O., Riley, E. P., & Wozniak, J. R. (2017). Cortical gyrification is abnormal in children with prenatal alcohol exposure. *NeuroImage: Clinical*, *15*. https://doi.org/10.1016/j.nicl.2017.05.015

10. Sawada Feldman, H., Lyons Jones, K., Lindsay, S., Slymen, D., Klonoff-Cohen, H., Kao, K., Rao, S., & Chambers, C. (2012). Prenatal Alcohol Exposure Patterns and Alcohol-Related Birth Defects and Growth Deficiencies: A Prospective Study. *Alcoholism: Clinical and Experimental Research*, *36*(4). https://doi.org/10.1111/j.1530-0277.2011.01664.x

11. de Filippis, L., Halikere, A., McGowan, H., Moore, J. C., Tischfield, J. A., Hart, R. P., & Pang, Z. P. (2016). Ethanol-mediated activation of the NLRP3 inflammasome in iPS cells and iPS cells-derived neural progenitor cells. *Molecular Brain*, *9*(1). https://doi.org/10.1186/s13041-016-0221-7

12. Sánchez-Alvarez, R., Gayen, S., Vadigepalli, R., & Anni, H. (2013). Ethanol Diverts Early Neuronal Differentiation Trajectory of Embryonic Stem Cells by Disrupting the Balance of Lineage Specifiers. *PLoS ONE*, *8*(5). https://doi.org/10.1371/journal.pone.0063794

13. Veazey, K. J., Carnahan, M. N., Muller, D., Miranda, R. C., & Golding, M. C. (2013). Alcohol-Induced Epigenetic Alterations to Developmentally Crucial Genes Regulating Neural Stemness and Differentiation. *Alcoholism: Clinical and Experimental Research*, *37*(7). https://doi.org/10.1111/acer.12080

14. Valenzuela, C. F., Puglia, M. P., & Zucca, S. (2011). Focus on: neurotransmitter systems. *Alcohol Research & Health : The Journal of the National Institute on Alcohol Abuse and Alcoholism*, *34*(1).

15. Halder, D., Mandal, C., Lee, B., Lee, J., Choi, M., Chai, J., Lee, Y., Jung, K., & Chai, Y. (2015). PCDHB14- and GABRB1-like nervous system developmental genes are altered during early neuronal differentiation of NCCIT cells treated with ethanol. *Human & Experimental Toxicology*, *34*(10). https://doi.org/10.1177/0960327114566827

16. Guizzetti, M., Moore, N. H., Giordano, G., VanDeMark, K. L., & Costa, L. G. (2010). Ethanol inhibits neuritogenesis induced by astrocyte muscarinic receptors. *Glia*, *58*(12). https://doi.org/10.1002/glia.21015

17. Mews, P., Egervari, G., Nativio, R., Sidoli, S., Donahue, G., Lombroso, S. I., Alexander, D. C., Riesche, S. L., Heller, E. A., Nestler, E. J., Garcia, B. A., & Berger, S. L. (2019). Alcohol metabolism contributes to brain histone acetylation. *Nature*, *574*(7780). https://doi.org/10.1038/s41586-019-1700-7

18. Zhao, X., & Bhattacharyya, A. (2018). Human Models Are Needed for Studying Human Neurodevelopmental Disorders. *The American Journal of Human Genetics*, *103*(6). https://doi.org/10.1016/j.ajhg.2018.10.009

19. Arzua, T., Yan, Y., Jiang, C., Logan, S., Allison, R. L., Wells, C., Kumar, S. N., Schäfer, R., & Bai, X. (2020). Modeling alcohol-induced neurotoxicity using human induced pluripotent stem cell-derived three-dimensional cerebral organoids. *Translational Psychiatry*, *10*(1). https://doi.org/10.1038/s41398-020-01029-4

20. Camp, J. G., Badsha, F., Florio, M., Kanton, S., Gerber, T., Wilsch-Bräuninger, M., Lewitus, E., Sykes, A., Hevers, W., Lancaster, M., Knoblich, J. A., Lachmann, R., Pääbo, S., Huttner, W. B., & Treutlein, B. (2015). Human cerebral organoids recapitulate gene expression programs of fetal neocortex development. *Proceedings of the National Academy of Sciences*, *112*(51). https://doi.org/10.1073/pnas.1520760112

21. Lancaster, M. A., Corsini, N. S., Wolfinger, S., Gustafson, E. H., Phillips, A. W., Burkard, T. R., Otani, T., Livesey, F. J., & Knoblich, J. A. (2017). Guided self-organization and cortical plate formation in human brain organoids. *Nature Biotechnology*, *35*(7). https://doi.org/10.1038/nbt.3906

22. Lancaster, M. A., Renner, M., Martin, C.-A., Wenzel, D., Bicknell, L. S., Hurles, M. E., Homfray, T., Penninger, J. M., Jackson, A. P., & Knoblich, J. A. (2013). Cerebral organoids model human brain development and microcephaly. *Nature*, *501*(7467). https://doi.org/10.1038/nature12517

23. Luo, C., Lancaster, M. A., Castanon, R., Nery, J. R., Knoblich, J. A., & Ecker, J. R. (2016). Cerebral Organoids Recapitulate Epigenomic Signatures of the Human Fetal Brain. *Cell Reports*, *17*(12). https://doi.org/10.1016/j.celrep.2016.12.001

24. Trujillo, C. A., Gao, R., Negraes, P. D., Gu, J., Buchanan, J., Preissl, S., Wang, A., Wu, W., Haddad, G. G., Chaim, I. A., Domissy, A., Vandenberghe, M., Devor, A., Yeo, G. W., Voytek, B., & Muotri, A. R. (2019). Complex Oscillatory Waves Emerging from Cortical Organoids Model Early Human Brain Network Development. *Cell Stem Cell*, *25*(4). https://doi.org/10.1016/j.stem.2019.08.002

25. Pașca, A. M., Park, J.-Y., Shin, H.-W., Qi, Q., Revah, O., Krasnoff, R., O'Hara, R., Willsey, A. J., Palmer, T. D., & Pașca, S. P. (2019). Human 3D cellular model of hypoxic brain injury of prematurity. *Nature Medicine*, *25*(5). https://doi.org/10.1038/s41591-019-0436-0

26. Quadrato, G., Nguyen, T., Macosko, E. Z., Sherwood, J. L., Min Yang, S., Berger, D. R., Maria, N., Scholvin, J., Goldman, M., Kinney, J. P., Boyden, E. S., Lichtman, J. W., Williams, Z. M., McCarroll, S. A., & Arlotta, P. (2017). Cell diversity and network dynamics in photosensitive human brain organoids. *Nature*, *545*(7652). https://doi.org/10.1038/nature22047

27. Trujillo, C. A., Adams, J. W., Negraes, P. D., Carromeu, C., Tejwani, L., Acab, A., Tsuda, B., Thomas, C. A., Sodhi, N., Fichter, K. M., Romero, S., Zanella, F., Sejnowski, T. J., Ulrich, H., & Muotri, A. R. (2021). Pharmacological reversal of synaptic and network pathology in human *MECP2* -KO neurons and cortical organoids. *EMBO Molecular Medicine*, *13*(1). https://doi.org/10.15252/emmm.202012523

28. Adams, J. W., Cugola, F. R., & Muotri, A. R. (2019). Brain Organoids as Tools for Modeling Human Neurodevelopmental Disorders. *Physiology*, *34*(5). https://doi.org/10.1152/physiol.00005.2019

29. Negraes, P. D., Trujillo, C. A., Yu, N.-K., Wu, W., Yao, H., Liang, N., Lautz, J. D., Kwok, E., McClatchy, D., Diedrich, J., de Bartolome, S. M., Truong, J., Szeto, R., Tran, T., Herai, R. H., Smith, S. E. P., Haddad, G. G., Yates, J. R., & Muotri, A. R. (2021). Altered network and rescue of human neurons derived from individuals with early-onset genetic epilepsy. *Molecular Psychiatry*. https://doi.org/10.1038/s41380-021-01104-2

30. Chailangkarn, T., Trujillo, C. A., Freitas, B. C., Hrvoj-Mihic, B., Herai, R. H., Yu, D. X., Brown, T. T., Marchetto, M. C., Bardy, C., McHenry, L., Stefanacci, L., Järvinen, A., Searcy, Y. M., DeWitt, M., Wong, W., Lai, P., Ard, M. C., Hanson, K. L., Romero, S., Jacobs, B., Dale, A. M., Dai, L., Korenberg, J. R., Gage, F. H., Bellugi, U., Halgren, E., Semendeferi, K., Muotri, A. R. (2016). A human neurodevelopmental model for Williams syndrome. *Nature*, *536*(7616). https://doi.org/10.1038/nature19067

31. Nageshappa, S., Carromeu, C., Trujillo, C. A., Mesci, P., Espuny-Camacho, I., Pasciuto, E., Vanderhaeghen, P., Verfaillie, C. M., Raitano, S., Kumar, A., Carvalho, C. M. B., Bagni, C., Ramocki, M. B., Araujo, B. H. S., Torres, L. B., Lupski, J. R., van Esch, H., & Muotri, A. R.

(2016). Altered neuronal network and rescue in a human MECP2 duplication model. *Molecular Psychiatry*, *21*(2). https://doi.org/10.1038/mp.2015.128

32. Vangipuram, S. D., Grever, W. E., Parker, G. C., & Lyman, W. D. (2008). Ethanol Increases Fetal Human Neurosphere Size and Alters Adhesion Molecule Gene Expression. *Alcoholism: Clinical and Experimental Research*, *32*(2). https://doi.org/10.1111/j.1530-0277.2007.00568.x

33. Dolganiuc, A. (2009). In vitro and in vivo models of acute alcohol exposure. *World Journal of Gastroenterology*, *15*(10). https://doi.org/10.3748/wjg.15.1168

34. Kigawa, Y., Hashimoto, E., Ukai, W., Ishii, T., Furuse, K., Tsujino, H., Shirasaka, T., & Saito, T. (2014). Stem cell therapy: a new approach to the treatment of refractory depression. *Journal of Neural Transmission*, *121*(10). https://doi.org/10.1007/s00702-014-1194-2

35. Burd, L., Blair, J., & Dropps, K. (2012). Prenatal alcohol exposure, blood alcohol concentrations and alcohol elimination rates for the mother, fetus and newborn. *Journal of Perinatology*, *32*(9). https://doi.org/10.1038/jp.2012.57

36. Delatour, L. C., Yeh, P. W. L., & Yeh, H. H. (2020). Prenatal Exposure to Ethanol Alters Synaptic Activity in Layer V/VI Pyramidal Neurons of the Somatosensory Cortex. *Cerebral Cortex*, *30*(3). https://doi.org/10.1093/cercor/bhz199

37. Ikonomidou, C., Bittigau, P., Ishimaru, M. J., Wozniak, D. F., Koch, C., Genz, K., Price, M. T., Stefovska, V., Hörster, F., Tenkova, T., Dikranian, K., & Olney, J. W. (2000). Ethanol-Induced Apoptotic Neurodegeneration and Fetal Alcohol Syndrome. *Science*, *287*(5455). https://doi.org/10.1126/science.287.5455.1056

38. Granato, A., & Dering, B. (2018). Alcohol and the Developing Brain: Why Neurons Die and How Survivors Change. *International Journal of Molecular Sciences*, *19*(10). https://doi.org/10.3390/ijms19102992

39. Anthony, B., Zhou, F. C., Ogawa, T., Goodlett, C. R., & Ruiz, J. (2008). Alcohol exposure alters cell cycle and apoptotic events during early neurulation. *Alcohol and Alcoholism*, *43*(3). https://doi.org/10.1093/alcalc/agm166

40. Sadrian, B., Wilson, D., & Saito, M. (2013). Long-Lasting Neural Circuit Dysfunction Following Developmental Ethanol Exposure. *Brain Sciences*, *3*(4). https://doi.org/10.3390/brainsci3020704

41. Kroener, S., Mulholland, P. J., New, N. N., Gass, J. T., Becker, H. C., & Chandler, L. J. (2012). Chronic Alcohol Exposure Alters Behavioral and Synaptic Plasticity of the Rodent Prefrontal Cortex. *PLoS ONE*, *7*(5). https://doi.org/10.1371/journal.pone.0037541

42. Saito, M., Chakraborty, G., Hui, M., Masiello, K., & Saito, M. (2016). Ethanol-Induced Neurodegeneration and Glial Activation in the Developing Brain. *Brain Sciences*, *6*(3). https://doi.org/10.3390/brainsci6030031

43. Slavney, P. R., & Grau, J. G. (1978). Fetal alcohol damage and schizophrenia. *The Journal of Clinical Psychiatry*, *39*(10).

44. Araujo, I., Henriksen, A., Gamsby, J., & Gulick, D. (2021). Impact of Alcohol Abuse on Susceptibility to Rare Neurodegenerative Diseases. *Frontiers in Molecular Biosciences*, *8*. https://doi.org/10.3389/fmolb.2021.643273

45. Medina, A. E. (2011). Fetal Alcohol Spectrum Disorders and Abnormal Neuronal Plasticity. *The Neuroscientist*, *17*(3). https://doi.org/10.1177/1073858410383336

46. Muralidharan, P., Sarmah, S., Zhou, F., & Marrs, J. (2013). Fetal Alcohol Spectrum Disorder (FASD) Associated Neural Defects: Complex Mechanisms and Potential Therapeutic Targets. *Brain Sciences*, *3*(4). https://doi.org/10.3390/brainsci3020964

47. Sawada Feldman, H., Lyons Jones, K., Lindsay, S., Slymen, D., Klonoff-Cohen, H., Kao, K., Rao, S., & Chambers, C. (2012). Prenatal Alcohol Exposure Patterns and Alcohol-Related Birth Defects and Growth Deficiencies: A Prospective Study. *Alcoholism: Clinical and Experimental Research*, *36*(4). https://doi.org/10.1111/j.1530-0277.2011.01664.x

48. Astley, S. J., Aylward, E. H., Olson, H. C., Kerns, K., Brooks, A., Coggins, T. E., Davies, J., Dorn, S., Gendler, B., Jirikowic, T., Kraegel, P., Maravilla, K., & Richards, T. (2009). Magnetic Resonance Imaging Outcomes From a Comprehensive Magnetic Resonance Study of Children With Fetal Alcohol Spectrum Disorders. *Alcoholism: Clinical and Experimental Research*, *33*(10). https://doi.org/10.1111/j.1530-0277.2009.01004.x

49. Lebel, C., Roussotte, F., & Sowell, E. R. (2011). Imaging the Impact of Prenatal Alcohol Exposure on the Structure of the Developing Human Brain. *Neuropsychology Review*, *21*(2). https://doi.org/10.1007/s11065-011-9163-0

50. Hampel, H., Mesulam, M.-M., Cuello, A. C., Farlow, M. R., Giacobini, E., Grossberg, G. T., Khachaturian, A. S., Vergallo, A., Cavedo, E., Snyder, P. J., & Khachaturian, Z. S. (2018). The cholinergic system in the pathophysiology and treatment of Alzheimer's disease. *Brain*, *141*(7). https://doi.org/10.1093/brain/awy132

51. Wozniak, J. R., Fuglestad, A. J., Eckerle, J. K., Kroupina, M. G., Miller, N. C., Boys, C. J., Brearley, A. M., Fink, B. A., Hoecker, H. L., Zeisel, S. H., & Georgieff, M. K. (2013). Choline supplementation in children with fetal alcohol spectrum disorders has high feasibility and tolerability. *Nutrition Research*, *33*(11). https://doi.org/10.1016/j.nutres.2013.08.005

52. Cacabelos, R. (2007). Donepezil in Alzheimer's disease: From conventional trials to pharmacogenetics. *Neuropsychiatric Disease and Treatment*, *3*(3).

53. Ballinger, E. C., Schaaf, C. P., Patel, A. J., de Maio, A., Tao, H., Talmage, D. A., Zoghbi, H. Y., & Role, L. W. (2019). Mecp2 Deletion from Cholinergic Neurons Selectively Impairs Recognition Memory and Disrupts Cholinergic Modulation of the Perirhinal Cortex. *Eneuro*, *6*(6). https://doi.org/10.1523/ENEURO.0134-19.2019

54. Zhao, X., Kuryatov, A., Lindstrom, J. M., Yeh, J. Z., & Narahashi, T. (2001). Nootropic Drug Modulation of Neuronal Nicotinic Acetylcholine Receptors in Rat Cortical Neurons. *Molecular Pharmacology*, *59*(4). https://doi.org/10.1124/mol.59.4.674

55. Wishka, D. G., Walker, D. P., Yates, K. M., Reitz, S. C., Jia, S., Myers, J. K., Olson, K. L., Jacobsen, E. J., Wolfe, M. L., Groppi, V. E., Hanchar, A. J., Thornburgh, B. A., Cortes-Burgos, L. A., Wong, E. H. F., Staton, B. A., Raub, T. J., Higdon, N. R., Wall, T. M., Hurst, R. S., … Rogers, B. N. (2006). Discovery of N -[(3 R)-1-Azabicyclo[2.2.2]oct-3-yl]furo[2,3-

c]pyridine-5-carboxamide, an Agonist of the α7 Nicotinic Acetylcholine Receptor, for the Potential Treatment of Cognitive Deficits in Schizophrenia: Synthesis and Structure−Activity Relationship. *Journal of Medicinal Chemistry*, *49*(14). https://doi.org/10.1021/jm0602413

56. Bunn, R. C., King, W. D., Winkler, M. K., & Fowlkes, J. L. (2005). Early Developmental Changes in IGF-I, IGF-II, IGF Binding Protein-1, and IGF Binding Protein-3 Concentration in the Cerebrospinal Fluid of Children. *Pediatric Research*, *58*(1). https://doi.org/10.1203/01.PDR.0000156369.62787.96

57. Labandeira-Garcia, J. L., Costa-Besada, M. A., Labandeira, C. M., Villar-Cheda, B., & Rodríguez-Perez, A. I. (2017). Insulin-Like Growth Factor-1 and Neuroinflammation. *Frontiers in Aging Neuroscience*, *9*. https://doi.org/10.3389/fnagi.2017.00365

58. Song, Y., Pimentel, C., Walters, K., Boller, L., Ghiasvand, S., Liu, J., Staley, K. J., & Berdichevsky, Y. (2016). Neuroprotective levels of IGF-1 exacerbate epileptogenesis after brain injury. *Scientific Reports*, *6*(1). https://doi.org/10.1038/srep32095

59. Costales, J., & Kolevzon, A. (2016). The therapeutic potential of insulin-like growth factor-1 in central nervous system disorders. *Neuroscience & Biobehavioral Reviews*, *63*. https://doi.org/10.1016/j.neubiorev.2016.01.001

60. Colangelo, C., Shichkova, P., Keller, D., Markram, H., & Ramaswamy, S. (2019). Cellular, Synaptic and Network Effects of Acetylcholine in the Neocortex. *Frontiers in Neural Circuits*, *13*. https://doi.org/10.3389/fncir.2019.00024

61. Picciotto, M. R., Higley, M. J., & Mineur, Y. S. (2012). Acetylcholine as a Neuromodulator: Cholinergic Signaling Shapes Nervous System Function and Behavior. *Neuron*, *76*(1). https://doi.org/10.1016/j.neuron.2012.08.036

62. Yoshiyama, Y., Kojima, A., Ishikawa, C., & Arai, K. (2010). Anti-Inflammatory Action of Donepezil Ameliorates Tau Pathology, Synaptic Loss, and Neurodegeneration in a Tauopathy Mouse Model. *Journal of Alzheimer's Disease*, *22*(1). https://doi.org/10.3233/JAD-2010-100681

63. Getachew, B., Hudson, T., Heinbockel, T., Csoka, A. B., & Tizabi, Y. (2018). Protective Effects of Donepezil Against Alcohol-Induced Toxicity in Cell Culture: Role of Caspase-3. *Neurotoxicity Research*, *34*(3). https://doi.org/10.1007/s12640-018-9913-3

64. Araujo, I., Henriksen, A., Gamsby, J., & Gulick, D. (2021). Impact of Alcohol Abuse on Susceptibility to Rare Neurodegenerative Diseases. *Frontiers in Molecular Biosciences*, *8*. https://doi.org/10.3389/fmolb.2021.643273

65. Subramoney, S., Eastman, E., Adnams, C., Stein, D. J., & Donald, K. A. (2018). The Early Developmental Outcomes of Prenatal Alcohol Exposure: A Review. *Frontiers in Neurology*, *9*. https://doi.org/10.3389/fneur.2018.01108

66. Dezonne, R. S., Sartore, R. C., Nascimento, J. M., Saia-Cereda, V. M., Romão, L. F., Alves-Leon, S. V., de Souza, J. M., Martins-de-Souza, D., Rehen, S. K., & Gomes, F. C. A. (2017). Derivation of Functional Human Astrocytes from Cerebral Organoids. *Scientific Reports*, *7*(1). https://doi.org/10.1038/srep45091

67. Porciúncula, L. O., Goto-Silva, L., Ledur, P. F., & Rehen, S. K. (2021). The Age of Brain Organoids: Tailoring Cell Identity and Functionality for Normal Brain Development and Disease Modeling. *Frontiers in Neuroscience*, *15*. https://doi.org/10.3389/fnins.2021.674563